Tellus (1996), 48B, 613–625
Printed in UK – all rights reserved

TELLUS
ISSN 0280–6509

The sensitivity of deduced CO_2 sources and sinks to variations in transport and imposed surface concentrations

By RACHEL LAW*[1] and IAN SIMMONDS, *School of Earth Sciences, University of Melbourne, Parkville, 3052, Australia*

(Manuscript received 25 July 1995; in final form 29 January 1996)

ABSTRACT

Carbon dioxide measurements exhibit substantial interannual variability in the growth rate and spatial distribution of CO_2 in the atmosphere. Here we consider typical variations in surface spatial distribution and year to year variability in transport and deduce what changes are required to the source and sink distributions of CO_2 to account for these variations. We use a three-dimensional (3d) tracer transport model with imposed surface CO_2 concentrations to deduce the sources required for consistency with these concentrations. Experiments have been conducted in which the tracer model winds and prescribed surface concentrations were varied and the impact on the sources assessed. The results indicate that changes to the transport (even in an extreme ENSO year) have only a small impact on the derived sources compared with the impact resulting from changes in the imposed concentrations. This could imply that the observed year to year variability in the annual mean spatial distribution of CO_2 results from changes in the CO_2 source distributions rather than changes in the transport.

1. Introduction

Predicting future global warming due to the enhanced greenhouse effect necessitates a good understanding of the carbon cycle. Carbon dioxide is constantly added to and removed from the atmosphere by exchange with the oceans and biosphere. In addition, there are anthropogenic perturbations to the natural cycle through the burning of fossil fuels and changes in land use. To assess the impact of these various sources and sinks, CO_2 levels are monitored at a number of surface locations globally. The longest records, dating from the late-1950s at the South Pole and Mauna Loa (20°N, 240°E), give a good indication of global CO_2 increases (Keeling and Whorf, 1994). The larger network of monitoring sites established over the last 10–15 years has allowed an appreciation of the spatial distribution of CO_2. This can be used to infer CO_2 sources which are generally difficult to measure directly. There are a number of ways of doing this inverse process of deducing sources from concentration data including 'synthesis' and 'mass-balance' methods.

The synthesis method involves estimating the distribution of each source process, for example fossil fuel burning, and using a transport model to determine the spatial distribution of CO_2 concentration associated with that source. Plausible combinations of sources are then established so that the sum of the calculated concentration fields matches the observed concentrations.

The seasonal component of the observations has been used to determine the seasonal transfer of CO_2 with the biosphere (Fung et al. 1983,

[1] Corresponding author.
* Present affiliation: Cooperative Research Centre for Southern Hemisphere Meteorology, Monash University, Clayton, Victoria 3168, Australia.

1987). Complete sets of sources have been determined by Keeling et al. (1989b) and Tans et al. (1990). Keeling et al. found that an oceanic sink was necessary in the northern high latitudes, to be consistent with their modelling and analysis of isotopic data. A contrasting view was given by Tans et al. who suggested that the observed partial pressures of CO_2 in the northern oceans are not consistent with a large oceanic CO_2 sink and hence the CO_2 must be absorbed by the terrestrial ecosystems. The synthesis methodology was extended by Enting et al. (1993, 1995) who used a Bayesian technique to establish source combinations. This method includes a constraint on the sources to be 'close' to prior estimates of their magnitudes and also allows uncertainty estimates to be placed on the sources. They found that global CO_2 and $^{13}CO_2$ growth rates are the most important elements of the observational data for reducing the uncertainties in the global budget.

The major disadvantage of the synthesis approach is the need to define the spatial distribution of each source process. While this is fairly well known for fossil fuel burning, it is less certain for such components as sources and sinks due to land use change or possible CO_2 fertilisation of the biosphere.

In the mass-balance method, the surface CO_2 concentrations are prescribed in the transport model and sources and sinks are deduced based on the model's transport. This has more commonly been done using two-dimensional (2d) models because of the difficulty in defining a global CO_2 distribution from the current network of monitoring sites. Examples include the studies of Enting and Mansbridge (1989, 1991) who assumed a steady state case and Tans et al. (1989) who tracked interannual variations. They obtained broadly similar results in suggesting a relatively small southern ocean sink of carbon, a source region through the tropics and, after subtracting the industrial CO_2 source, a northern hemisphere carbon sink. The seasonality of the sources was discussed in both papers while Tans et al. also assessed the impact on the calculated sources of using CO_2 concentration data from 1982–83, a strong El Niño event. Conway et al. (1994) extended the work of Tans et al. (1989) using longer observed CO_2 time series while Ciais et al. (1995) used the ratio of $^{13}CO_2$ to $^{12}CO_2$ to discriminate between biosphere and ocean fluxes. Sources have been calculated using three-dimensional models, either by assuming no longitudinal variation in concentration (Law et al., 1992) or by only constraining the surface zonal mean concentrations (Rayner and Sarmiento, 1993). The results are qualitatively similar to those from the 2d models.

As the amount of CO_2 data has increased, it has become apparent that there is significant interannual variability in the growth rate, seasonal cycle and spatial distribution of surface CO_2 concentration. Many authors (Keeling et al., 1989a; Dargaville and Simmonds, 1993) have commented on the consistency of growth rate anomalies across the global monitoring network. This would tend to imply that the variation is due to changes in sources rather than changes in transport (Gaudry et al., 1991). A number of authors including Bacastow (1976) have linked the growth rate with the Southern Oscillation Index (SOI); the growth rate appears to be higher during an El Niño-Southern Oscillation (ENSO) event. Many studies have tried to establish the mechanism behind this result (e.g. Newell and Weare, 1977; Newell et al., 1978, Thompson et al., 1986, Elliot et al., 1991). Keeling et al. (1989a) and Francey et al. (1995) used atmospheric carbon isotope data to distinguish between the biospheric and oceanic contributions to the interannual variability of the global CO_2 budget. Less work has been done on the impact of ENSO on the spatial distribution of CO_2 although we might expect this to be large; ENSO is associated with large global-scale circulation anomalies of both ocean and atmosphere and impacts on biotic activity. Conway et al. (1988) suggested that ENSO events will have an impact on the interhemispheric CO_2 gradient. Their analysis of 1981–84 data showed that the 'normal' equatorial local maximum concentration was missing in 1982. They linked this to an anomaly in the equatorial CO_2 source. It is worth noting here that little work has been done on the impact of interannual variability of transport since most tracer models have been used with only one year of forcing winds. It is important in our understanding of the interannual variability in CO_2 spatial distribution that we consider interannual variability of both sources *and* transport.

In this paper, we use the mass-balance method of calculating CO_2 sources to investigate the interannual variability in the spatial distribution

of CO_2 concentrations. A comparison is made of the impact of changes in transport with changes in the imposed CO_2 concentrations. The mass-balance method using a three-dimensional transport model forced with zonally uniform concentration is chosen for a number of reasons. No prior assumptions are required about carbon budgets or the spatial distributions of sources in order to calculate the sources. The inverse problem is more sensitive than the forward problem since small scale features are amplified rather than diminished and hence there is the potential to learn more about the source distribution. Additionally, there has been little use of 3d models (which should represent CO_2 transport better than 2d models) for mass-balance studies compared with their fairly extensive use in synthesis studies. One limitation of the mass-balance method for CO_2 is that while a complete source field is determined, this provides no direct information on which processes contribute to the source distribution.

2. Model and method

The tracer model used in this study is derived from the Melbourne University General Circulation Model (GCM) (Simmonds, 1985; Simmonds et al., 1988) and has been described by Law et al. (1992). The model solves the tracer continuity equation using daily GCM winds as input (there is no diurnal cycle). The model fields are described spectrally with rhomboidal, 21 wave resolution at 9 vertical levels. The offline tracer model has been compared with an 'on-line' version of the model, in which the winds are known at each timestep. The difference between online and offline versions is small compared to the range of results obtained from a tracer model intercomparison (Rayner and Law, 1995) which suggests that the offline tracer model adequately reproduces the online tracer transport. Convective transport is parameterised as in Law et al. (1992) except that daily statistics rather than monthly statistics of convection events have been used. The tracer concentration at any height is adjusted towards the vertical mean concentration by an amount dependent on the number and nature of convection events at that location.

We impose surface CO_2 concentrations in the tracer model and deduce the sources consistent with these concentrations and the transport effected by the input winds. The tracer model is initialised with a CO_2 distribution that is constant in longitude and height. After each timestep the source or sink required to maintain the 'observed' concentrations is calculated as the difference between the modelled surface concentrations and those imposed. The simulation of the rest of the atmosphere is unconstrained.

This method assumes that all CO_2 sources and sinks are located at the surface. However the oxidation of CO produces CO_2 throughout the troposphere. The impact that this will have on the calculated sources and sinks is discussed by Enting and Newsam (1990) and Enting and Mansbridge (1991), who use a global oxidation source of 0.86 $GtCyr^{-1}$. They show that the calculated surface sources will be over-estimated to compensate if this source is neglected. The spatial structure of the error will be dependent on both the distribution of the oxidation source, which has maximum values in the tropics, and the circulation which will tend to spread the impact of this distribution. Hence the assumption of only surface sources and sinks introduces small uncertainties into the sources calculated here.

Initial results using this method were given in Law et al. (1992). Here we present a number of extensions to that work. Sources have been calculated using a full annual cycle of winds and CO_2 concentrations, including more than one year of GCM wind data. Experiments using one month of winds perpetually, as in Law et al. (1992), have also been performed with a variety of wind fields and CO_2 annual mean distributions to examine the sensitivity of the deduced sources.

3. Impact on sources of variations in the forcing winds

3.1. Experiment details

We describe first the experiment using the full annual cycle. The model was run for six years. For the first three years the tracer model was forced with wind and convection data from year 4 of a ten year GCM control run (forced with climatological sea surface temperatures). This was to allow the model time to build up a quasi-steady vertical profile of CO_2, given that it is initialised with no vertical variation. Years 4 and 5 of the

tracer model run were forced with wind and convection data from years 5 and 6 of the control GCM run respectively while the final year used wind data from year 4 and convection data from year 6. It is important to check how much variation there is in sources derived from different years of control winds and convection. The final year of the experiment was designed to assess whether the wind or the convection data has a stronger influence on the sources.

The CO_2 surface concentrations used to force the model comprise a seasonal cycle (varying in latitude only) and a linear trend of 1.5 ppmv yr^{-1}. The imposed concentrations for the first year of the experiment are shown in Fig. 1. They have been linearly interpolated to the grid used by the tracer model from the spline fit to the CO_2 data produced by Enting and Mansbridge (1991) (hereafter referred to as E&M). This was designed to be representative of an 'average' year. The seasonal cycle is described by the first two components of a Fourier series. The concentrations are assumed to be uniform with longitude because it is not possible to define longitudinal CO_2 variations from the current monitoring network. We assume that since CO_2 data is collected in 'remote' locations the concentrations obtained are zonally representative and thus a mean north-south CO_2 profile can be obtained. We will discuss this assumption later. This means that we expect only the zonal average of our calculated sources to give meaningful results and hence this will be the focus of our discussion. The global mean is removed from the data set before running the experiment as this minimises the effects of any numerical inaccuracies in tracer mass conservation.

3.2. *Vertical structure*

The model is initialised with vertically-constant CO_2 values after which time the concentrations away from the surface are free to respond to

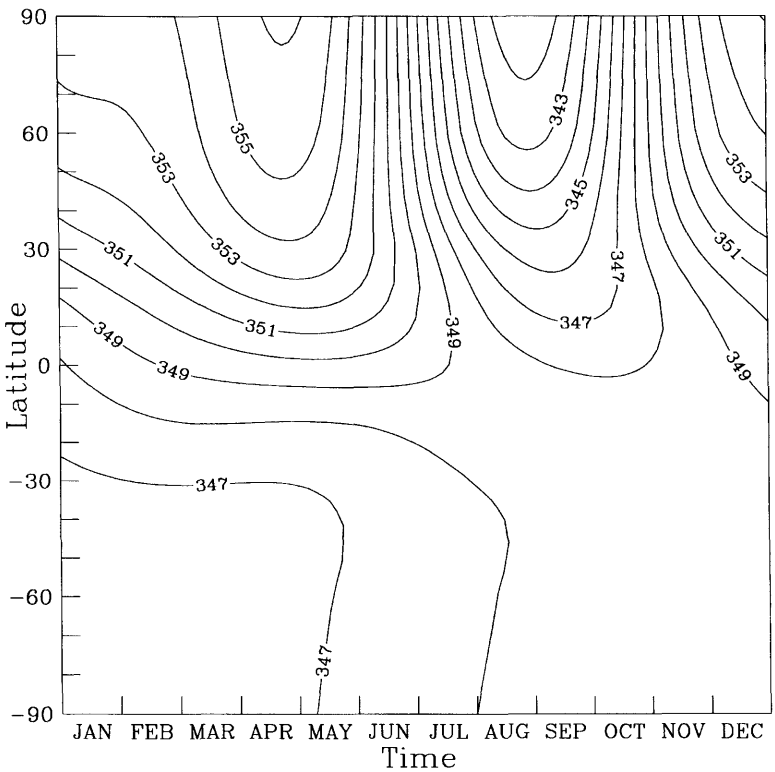

Fig. 1. Annual cycle of surface CO_2 concentrations from Enting and Mansbridge (1991) plus a trend of 1.5 ppmv yr^{-1}.

atmospheric mixing and the surface constraint. Comparing the distribution obtained with upper air CO_2 observations provides an indication of the quality of the model simulation. For this comparison, we use the CO_2 distributions from the third year of the experiment but the distributions for the following years are very similar. Two cross-sections are shown in Fig. 2, the first gives the zonally-averaged annual mean concentration and the second a measure of the amplitude of the seasonal cycle. The value plotted is the concentration difference between the maximum and minimum monthly and zonally averaged concentrations at each height and latitude.

The annual mean concentrations (Fig. 2a) decrease with height in the northern hemisphere troposphere with the opposite occurring in the south. This is indicative of higher concentration air from the northern hemisphere moving into the southern hemisphere in the upper troposphere;

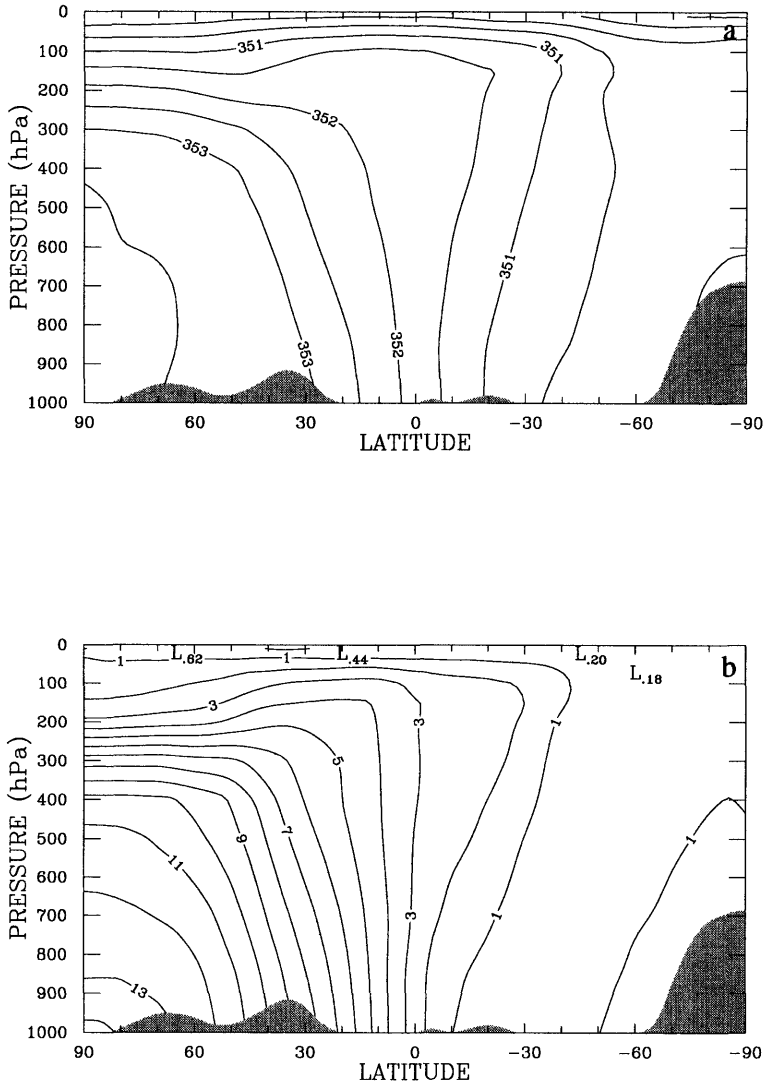

Fig. 2. Zonally averaged CO_2 concentration (a) and peak-to-peak amplitude of the seasonal cycle (b). The contour intervals are 0.5 and 1.0 ppmv respectively.

northern hemisphere air is lifted in the tropics and then brought southwards by the upper branch of the southern Hadley cell. The cross-section of the seasonal range of CO_2 concentration (Fig. 2b) shows that the largest amplitudes occur in the northern troposphere decreasing with height from the surface. The decrease with height is relatively rapid at high latitudes but smaller in the low and mid-latitudes. In this region the amplitudes are only 1–2 ppmv lower at 300 hPa than at the surface. The amplitudes are significantly smaller in the stratosphere; the region of rapid decrease in the amplitude indicates the 'capping' effect of the tropopause. The cross-section shows one region of increasing amplitude with height between 0–40°S. As before this reflects the mixing of air with northern hemisphere characteristics into the upper troposphere of the southern hemisphere.

Three aspects of these results can be compared to the upper air observations of Pearman and Beardsmore (1984) and Nakazawa et al. (1991): these are (i) the vertical gradient in the tropics and mid-latitudes, (ii) the north-south distribution of annual mean concentration in the upper troposphere and (iii) the seasonal amplitudes in the southern mid-latitudes. Nakazawa et al. (1991) present upper and lower tropospheric concentrations for 40°N to 30°S; the model simulation generally underestimates the CO_2 concentration difference between these heights. The model shows some consistency with the observations for the location of the maximum concentration in the upper troposphere (0–10°N) but the decrease in concentration away from the equator is smaller to the north and larger to the south than observed. The aircraft data of Pearman and Beardsmore (1984) for the Tasman Sea (40°S) region give amplitudes of 2–3 and 1.2 ppmv for the upper and mid-troposphere respectively, somewhat larger than are modelled.

There are at least three possible contributions to the discrepancies between the model results and observations: the appropriateness of the comparison, transport error and uncertainty in the prescribed surface values. The first involves the differences introduced by comparing zonal mean model results forced with zonally uniform surface concentrations to observations from specific locations, predominantly around the West Pacific. It is difficult to assess how much of the difference this accounts for although we might expect it to be small, at least in the upper troposphere where the surface sources are remote and mixing is relatively rapid.

A second contribution is from uncertainties in the modelled transport and, in particular, the possibility that the model vertical mixing processes are too strong. A recent intercomparison of tracer transport models (Rayner and Law, 1995) has shown that this model's mixing is slightly faster than most other models involved in the comparison. To assess the impact on the upper troposphere concentrations of the treatment of convective mixing, the model experiment was repeated with no convective transport (and the year-4 control winds). The difference in upper and lower tropospheric mean concentrations is closer to the observed value in the northern hemisphere but there is little change in the south. The values for the southern upper troposphere seasonal ranges are slightly larger but are still significantly smaller than the limited observations indicate. However it is important to note that the lack of convective mixing will tend to be compensated for by an increase in transport due to vertical diffusion.

It may be that the discrepancy with the observations results as much from the choice of surface boundary condition as from uncertainties in the model transport. For example, a larger seasonal cycle in the imposed surface concentrations would result in larger amplitudes throughout the atmosphere. Conway et al. (1994) give observed peak-to-peak amplitudes of 15–19 ppmv for sites north of 50°N which is higher than the 11–14 ppmv used here. In addition, forward simulations (Fung et al., 1983, 1987; Heimann et al., 1989) using estimates of the seasonal biospheric source give substantially larger amplitudes over land surfaces (20–25 ppmv) than are measured at the, predominantly ocean-based, remote monitoring stations. This would suggest that there is potential for larger seasonal cycles in the imposed concentrations. Similarly the north-south surface concentration gradient could be underestimated based on the current network of monitoring stations which are generally remote from the fossil fuel sources.

In general, the vertical structure of modelled concentration shows the same basic features as seen in CO_2 aircraft observations. However, CO_2 gradients, particularly in the vertical direction, appear to be smaller than observed. If this is, at

least partly, a result of over-efficient vertical mixing, the sources deduced in the experiments will tend to be over-estimated; as CO_2 is more rapidly taken out of the surface layer, a larger source is required to maintain the surface concentrations.

3.3. *Sources*

The deduced sources for the third year of the experiment are shown, zonally and monthly averaged, in Fig. 3. The dominant feature is the seasonal variation in the northern hemisphere, with a large source through the winter months and a large sink in the summer. This is a response to the large amplitude seasonal cycle in northern hemisphere CO_2 concentrations, due to the uptake and release of CO_2 by the biosphere. Maximum sources and sinks occur in the northern mid-latitudes, slightly further south than in the estimate of the terrestrial biosphere fluxes by Fung et al. (1987). The timing of the peak values also differs from the Fung et al. estimates but both produce spring and autumn source maxima. A more detailed comparison is not possible because the sources and sinks presented here include all processes not just the terrestrial biosphere exchange. A CO_2 sink is maintained throughout the year in the southern mid-latitudes. This sink is strongest in late autumn and winter. The equatorial regions are a CO_2 source for most of the year. Enting and Mansbridge (1989) obtained broadly similar results using a two-dimensional model forced with GCM-derived circulation fields.

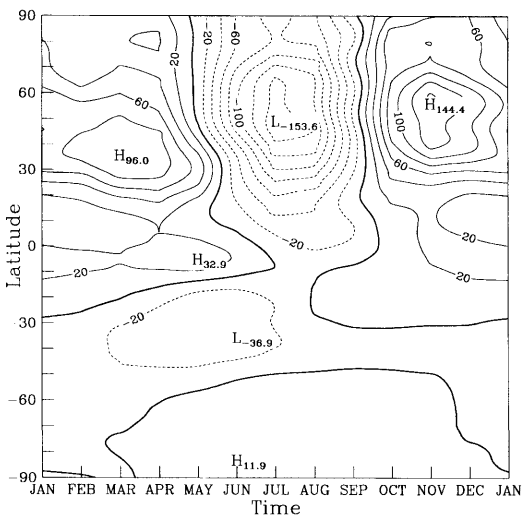

Fig. 3. Zonally and monthly averaged CO_2 source for year 3 of the experiment. The contour interval is 20 $gCm^{-2}yr^{-1}$.

The zonally-averaged annual mean sources for years 3, 4, 5 and 6 of the experiment are shown in Fig. 4 (Recall that years 3–5 use different GCM years of wind and convection data while year 6 is the mixed case). We find little variability and, in particular, simulate in all years sources through the northern hemisphere, tropics and high southern latitudes with a sink in the southern mid-latitudes. The integrated values for each of these regions are given in Table 1 along with those for the 'no convection' case. The sources calculated in the 'no convection' experiment tend to be smaller than those obtained with convection because the vertical CO_2 mass transport from the surface layer has been reduced. They indicate the typical change in magnitude of the deduced sources due to uncertainties in the model transport.

The northern hemisphere source reflects the CO_2 contribution from fossil fuel burning which is predominantly located in the northern mid-latitudes. The deduced source is not, however, large enough to account for all the fossil emissions produced in this area. This implies that there is a natural sink in this region. The tropical source may be linked to outgassing from the tropical

Table 1. *Regional annual mean sources in GtC* yr^{-1} *for years 3–6 of the experiment forced with different years of control GCM winds and for an experiment with no convective transport*

	Year 3	Year 4	Year 5	Year 6	No conv.
10–90°N	3.08	3.19	3.09	3.23	3.00
10°N–20°S	1.11	1.00	1.03	1.10	0.82
20–53°S	−1.19	−1.13	−1.12	−1.23	−0.81
53–90°S	0.15	0.14	0.13	0.17	0.12

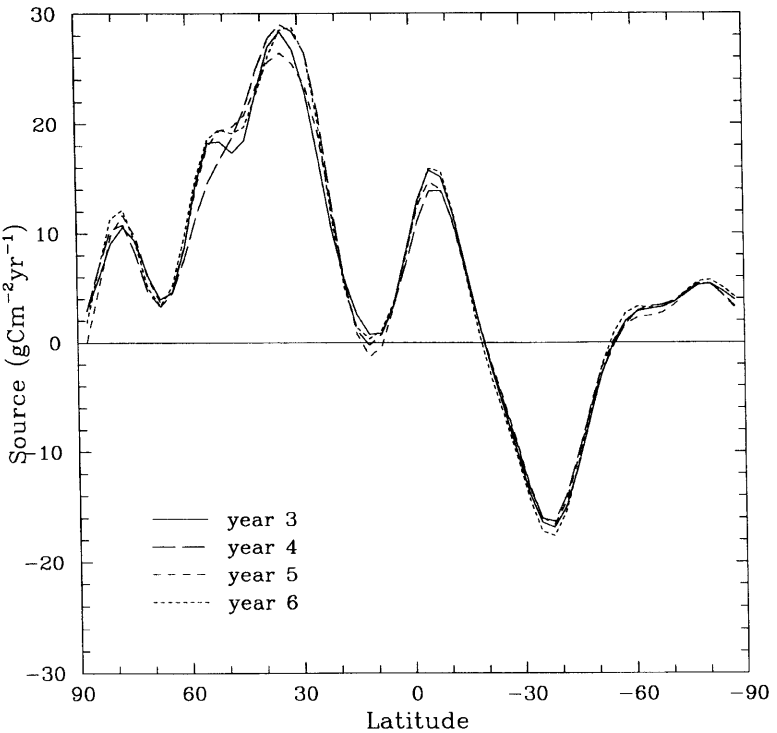

Fig. 4. Zonal annual mean CO_2 source in $gCm^{-2}yr^{-1}$. The key indicates which year of the experiment each curve applies to.

ocean with additional contributions from deforestation. In fact, the two processes combined are thought to be a larger source than the approximately 1 GtC calculated here (Takahashi, 1989; Houghton, 1991). This would suggest that a biotic sink also occurs in this region. The southern mid-latitude sink is due to uptake by the oceans. Ocean processes are also thought to account for the small source found in the high southern latitudes.

The small differences between the annual sources seen in Fig. 4 indicate that variations in transport within a control GCM experiment have little influence on the calculated sources. Thus sources can be reliably estimated using any one year of control winds. It is not obvious that the year with mixed wind and convection data (year 6) is more like either of the years run with one of the same data sets (years 3 and 5). This suggests that neither the variability in the winds or in the convection data dominates the (small) variability found in the deduced sources.

4. 1983 ENSO case. Contrast between impact of different winds and different imposed concentrations

The variation in transport in the previous experiment was limited by the use of winds from a control GCM experiment. In the following experiments, we investigate the impact on the derived sources of using winds that are typical of a strong ENSO event. This provides an example of the effect of using winds that are very different from the climatological mean and hence more representative of the extreme of realistic tests. We also compare this 'maximum' wind response with the response to changing the imposed surface concentrations.

The experiments have been performed under *perpetual* January conditions and the model is forced with the annual mean CO_2 'observations' to give an approximate annual mean source. Experiments (Law, 1993) indicate that the zonal

mean sources obtained using either January or July perpetual winds give a good first approximation to the sources obtained when using the complete annual cycle. The model is run for 217 days to remove any significant 'memory' of the initialisation. In this case the 1.5 ppmv yr^{-1} trend was not included.

The tracer model is run with two sets of winds: the January winds from year 4 of the control GCM run and the last 31 days from a perpetual January GCM run forced with the January 1983 SST data of Reynolds (1988). The difference between the SST-forced and control wind fields for 850 and 200 hPa has been compared with the difference between January 1983 and the 1980–1989 mean January from the analyses of the European Centre for Medium Range Weather Forecasts. The differences are broadly similar in magnitude and structure. There is some indication that the differences in the modelled meridional wind are slightly larger than those observed. Additionally, moderate zonal wind differences tend to extend throughout the tropical Pacific in the model whereas they are confined to the East Pacific in the analyses. There is some change in the distribution of convection between the 1983 SST and control runs. There is an increase in moist convective events around 20°S and a decrease around 10°N. The largest changes in dry convection occur between 0 and 30°N.

The tracer model was forced with three annual mean CO_2 distributions: the annual mean component of the E&M distribution described above and two different fits to observed annual mean NOAA flask concentrations for 1983 (Conway et al., 1991). The two fits used were the same spline fit (50% attenuation to variations whose wavelength was Δ sin(latitude)=1) as used in E&M and an eighth order polynomial fit in sine latitude. The three distributions are shown in Fig. 5 along with the 1983 data used. The scatter in the observed data illustrates the problems associated with assuming the data are zonally representative and how to appropriately fit that data. The two fits used here encompass a range of 'flexibility' to follow the scatter in the data which will provide an indication of the impact on the sources of the uncertainties in defining a meridional CO_2 distribution.

The zonal average of the deduced sources is shown in Fig. 6 for the last 31 day period of each

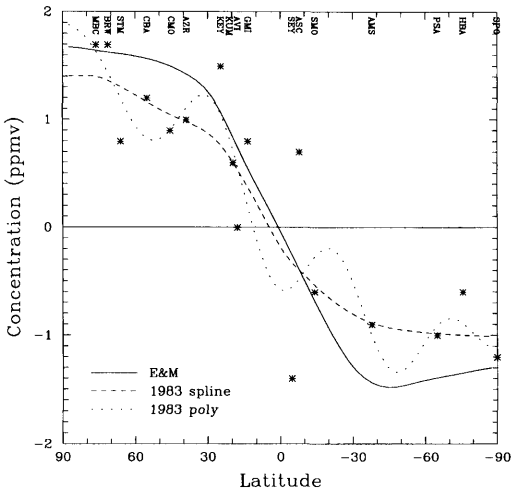

Fig. 5. CO_2 concentrations for 1983 for NOAA monitoring stations (*). The sites are identified at the top of the figure by the codes used in Conway et al. (1994). Also shown are spline and eighth order polynomial fits (in sine latitude) to this data and the annual mean distribution of Enting and Mansbridge (1991). The curves are identified in the key. The global mean concentration has been subtracted from the distributions and the data.

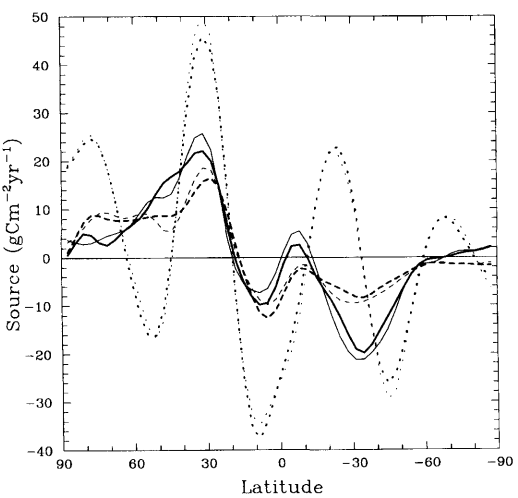

Fig. 6. Zonally averaged CO_2 sources for the seventh 31-day period of six January perpetual experiments; E&M imposed concentrations (solid), 1983 spline fit concentrations (dashed) and 1983 eighth order polynomial fit concentrations (dotted). The three concentration distributions were run with control (standard) and '1983' (bold) winds.

experiment and the integrated northern hemisphere source/southern hemisphere sink is given in Table 2. Since these experiments have no CO_2 trend, the global net source is zero and the net northern source balances the net southern hemisphere sink. Three relatively distinct source distributions are found depending on the CO_2 values imposed. In each case the impact of using different winds is relatively small. Those cases that used the E&M distribution produced sources which are very similar in structure to those obtained using the full annual cycle. The values are reduced by approximately 2–8 $gCm^{-2}yr^{-1}$ depending on latitude compared with the annual cycle results because the perpetual case was run without the 1.5 ppmv yr^{-1} CO_2 trend. There is some variation in the sources with the change in wind fields. For example, the southern mid-latitude sink is smaller using the '1983' winds whereas the equatorial sink is larger.

It is important to consider the relative contributions to this change by advective and sub-grid scale processes and in particular whether the sub-grid scale mixing could mask a larger impact on the sources due to the change in advection. To do this, the two cases with the E&M distribution have been repeated with no vertical diffusion or convection. The deduced sources are similar in the tropics but much smaller through the mid-latitudes where the sub-grid scale processes make a significant contribution to transport away from the surface. The impact of changing the winds is comparable to that in the full transport case. This suggests that even if the vertical sub-grid scale mixing in this model is too strong, it is not distorting the sensitivity to changing the wind and convection data.

The spline fit to the 1983 data produces a broadly similar source distribution although the magnitude of the southern mid-latitude sink is reduced substantially. The impact of the '1983' winds is consistent with that seen for the E&M distribution. The figure shows that even with a relatively inflexible fit that ignores much of the possible structure in the 1983 data, the impact of changing from an 'average' distribution is larger than that due to changing the forcing winds. This is also seen in the hemispherically integrated sources; the difference in source due to changing from control to 1983 winds (−0.13 GtC) is less than when changing from the E&M average distribution to the 1983 spline (−0.54 GtC).

Table 2. *Northern hemisphere source in GtC* yr^{-1} *for three different* CO_2 *distributions and two sets of winds*

	Control winds	1983 winds
E&M	1.86	1.73
spline	1.32	1.19
poly	0.64	0.33

The deduced source distribution is changed substantially, even on a hemispheric scale, when the eighth order polynomial fit is used. The sources and sinks estimated using this fit reflect the local maxima and minima in the concentration data. The maximum source strengths are larger due to the steeper gradients present in the polynomial distribution; these will tend to result in greater CO_2 transport and hence require larger sources to maintain the prescribed concentrations. Again, there is only a small change in the sources with the change in wind fields which suggests that the impact of the winds is not increased by allowing smaller scale structure in the CO_2 distribution.

This result illustrates the need to consider carefully the appropriateness of any particular fit to the data. A balance is required between a smooth fit that will produce a more robust set of sources and a more flexible fit which would more easily accommodate any interannual variability in CO_2 distribution. In the next section, we will examine this possibility of identifying 'real' interannual variability in the CO_2 sources and sinks. The above set of experiments, however, clearly shows that variations in the CO_2 sources have more potential to change the spatial distribution of CO_2 than changes in CO_2 transport.

5. Variation in sources derived from 9 years of CO_2 data

A further experiment has been run using monthly CO_2 data from 1982–1990. For each month the mean CO_2 concentrations from the NOAA flask data (Conway et al., 1991) have been fitted with a spline to describe the meridional distribution. The stiffness of the spline was chosen to give 50% attenuation to variations whose wavelength was Δ sin(latitude)=0.707. This provides

more flexibility than the spline used in the previous experiment and should reasonably represent interannual variability while maintaining a relatively smooth distribution.

The NOAA flask data were available for 14 (in 1982)-23 (in 1987/88) locations depending on the year. The Mauna Loa and Niwot Ridge data were not used because of the altitude of these sites. The annual mean CO_2 profiles are shown (as deviations from the global mean) in Fig. 7. The north-south gradient is larger towards the end of the period than in the early 1980s. The distributions show most variety through the northern mid and high latitudes.

Sources have been calculated by constraining the surface layer to the distribution fitted to the monthly means. This surface boundary condition is kept fixed throughout the month. The year-4 control GCM winds were used as in the previous experiments. The model was run for 11 years to include 2 years for the initialisation. The zonal annual mean sources are shown in Fig. 8. A remarkable feature of this figure is the large variations in the deduced sources with the changing imposed concentration distribution as we found for the ENSO 1983 case (Fig. 6). The southern mid-latitude sink is fairly persistent through each year though the magnitude of the sink varies somewhat. With the exception of 1983 all years indicate a source at the equator although again the magnitude varies widely. The northern hemisphere results are more varied, reflecting the high variability of the CO_2 distributions in this region.

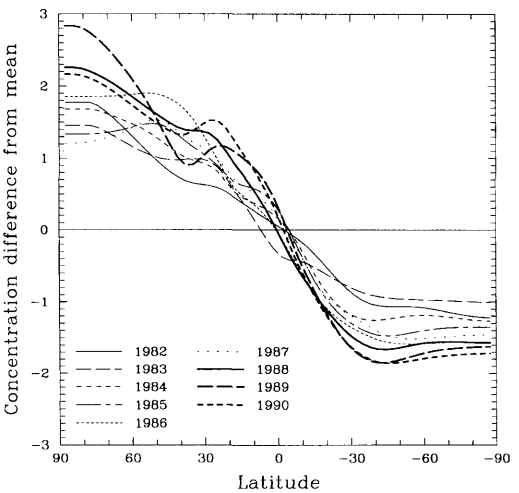

Fig. 7. Annual mean of spline fits (in sine latitude) to monthly CO_2 concentration data for 1982–1990. The global mean concentration has been subtracted from each distribution. The line identification is given in the key.

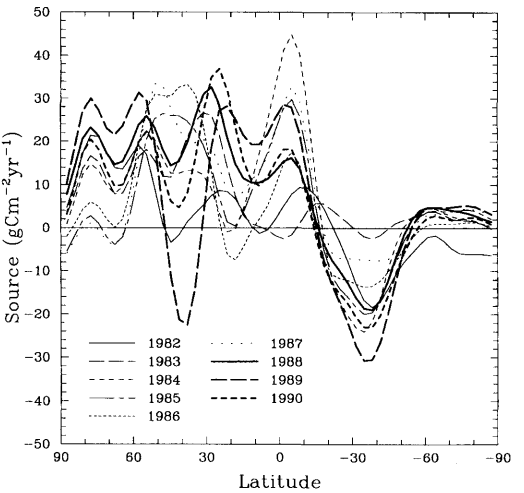

Fig. 8. Zonal annual mean CO_2 sources from an experiment forced with CO_2 distributions based on spline fits to monthly CO_2 data from 1982–1990. The line identification is given in the key.

Hemispheric and global mean sources are given in Table 3. These integrated values show the impact of both changes in the spatial distribution and variation in the CO_2 increase through this period. For example, 1985, 1987 and 1990 all have similar global net sources, indicating a similar CO_2 global increase in concentrations but they give very different hemispheric sources due to different imposed spatial distributions. The integrated sources show some agreement with those

Table 3. *Hemisphere and global annual mean sources in GtC yr^{-1}*

	N. hem	S. hem	Global
1982	1.51	−0.80	0.71
1983	3.06	0.38	3.44
1984	3.29	0.74	4.03
1985	3.36	−0.04	3.32
1986	3.03	−0.61	2.42
1987	2.19	1.09	3.28
1988	4.79	−0.49	4.30
1989	3.73	−1.01	2.72
1990	4.47	−1.20	3.27

calculated by Conway et al. (1994) using a two-dimensional model.

Identifying 'real' interannual variability in these sources is difficult. We expect El Niño events, which occurred in 1982/83 and 1987 to have a significant impact on the spatial distribution of sources and sinks but this is not clear from these results. 1982 and 1983 show smaller equatorial sources and 1983 and 1987 show reduced southern mid-latitude sinks but at best this is only suggestive of some ENSO link. It is likely that much of the variability seen is due to uncertainties in the data. For example, the northern mid-latitude sink in 1989 results from some low concentrations at Azores through the later part of 1989 which it may have been more appropriate not to use. Given the sensitivity of the sources to the prescribed concentrations, it is obviously important that any future source calculations examine questions such as the changing network size and whether the data should be considered as zonally representative.

6. Conclusions

A three-dimensional tracer model has been used to estimate CO_2 sources and sinks from information on surface concentrations. The seasonal variation in the imposed concentrations is reflected in the deduced sources. Thus the largest variation is in the northern mid-latitudes with winter sources and summer sinks. The annual mean shows northern hemisphere and tropical sources and a southern mid-latitude sink. This is consistent with the higher CO_2 concentrations found in the northern hemisphere relative to the southern hemisphere. The upper level concentrations simulated by the model agree reasonably with aircraft observations of CO_2 concentrations.

The model results are relatively insensitive to variations in the forcing circulation (winds and convection). The small impact of the wind data is true for both GCM winds calculated with climatological SSTs and those calculated with SSTs for a specific month and year. By contrast, the sources calculated using CO_2 distributions based on different years of CO_2 data show considerable differences. There are also large differences associated with how a meridional distribution is fitted to the surface observations. These uncertainties mean that, from these results, any link between the geographical distribution of the calculated sources and the occurrence of an El Niño event is tenuous. The large impact on the sources of the imposed CO_2 surface concentrations and the small impact of the forcing circulation suggests that variability in the observed north-south profile of annual mean CO_2 concentration is more likely to result from changes in the CO_2 source distribution than changes in the CO_2 transport.

7. Acknowledgements

We would like to thank Ian Enting and Peter Rayner for their helpful comments on this paper.

REFERENCES

Bacastow, R. B. 1976. Modulation of atmospheric carbon dioxide by the southern oscillation. *Nature* **261**, 116–118.

Ciais, P., Tans, P. P., White, J. W. C., Trolier, M., Francey, R. J., Berry, J. A., Randall, D. R., Sellers, P. J., Collatz, J. G. and Schimel, D. S. 1995. Partitioning of ocean and land uptake of CO_2 as inferred by $\delta^{13}C$ measurements from the NOAA Climate Monitoring and Diagnostics Laboratory Global Air Sampling Network. *J. Geophys. Res.* **100**, 5051–5070.

Conway, T. J., Tans, P., Waterman, L. S., Thoning, K. W., Masarie, K. A. and Gammon, R. H. 1988. Atmospheric carbon dioxide measurements in the remote global troposphere, 1981–1984. *Tellus* **40B**, 81–115.

Conway, T. J., Tans, P. P. and Waterman, L. S. 1991. Atmospheric CO_2 records from sites in the NOAA/CMDL air sampling network. *Trends '91. A Compendium of data on global change*, ed. Boden, T. A., Sepanski, R. J., Stoss, F. W. Carbon Dioxide Information Analysis Center, Oak Ridge, USA, 44–143.

Conway, T. J., Tans, P. P., Waterman, L. S., Thoning, K. W., Kitzis, D. R., Masarie, K. A. and Zhang, N. 1994. Evidence for interannual variability of the carbon cycle from the National Oceanic and Atmospheric Administration/Climate Monitoring and Diagnostics Laboratory Global Air Sampling Network. *J. Geophys. Res.* **99**, 22831–22855.

Dargaville, R. and Simmonds, I. 1993: Spatial consistency of short-term atmospheric carbon dioxide concentrations. *Proceedings of the 4th International Conference on Southern hemisphere meteorology and oceanography*. Hobart, Australia, March 1993, American Meteorological Society, 433–434.

Elliot, W. P., Angell, J. K. and Thoning, K. W. 1991. Relation of atmospheric CO_2 to tropical sea and air temperatures and precipitation. *Tellus* **43B**, 144–155.

Enting, I. G. and Mansbridge, J. V. 1989. Seasonal sources and sinks of atmospheric CO_2: Direct inversion of filtered data. *Tellus* **41B**, 111–126.

Enting, I. G. and Newsam, G. N. 1990. Inverse Problems in atmospheric constituent studies: II. Sources in the free atmosphere. *Inverse Problems* **6**, 349–362.

Enting, I. G. and Mansbridge, J. V. 1991. Latitudinal distribution of sources and sinks of CO_2: Results of an inversion study. *Tellus* **43B**, 156–170.

Enting, I. G., Trudinger, C. M., Francey, R. J. and Granek, H. 1993. *Synthesis inversion of atmospheric CO_2 using the GISS tracer transport model.* CSIRO Div. Atmos. Res. Tech. Paper No. 29, 44pp.

Enting, I. G., Trudinger, C. M. and Francey, R. J. 1995. A synthesis inversion of the concentration and $\delta^{13}C$ of atmospheric CO_2. *Tellus* **47B**, 35–52.

Francey, R. J., Tans, P. P., Allison, C. E., Enting, I. G., White, J. W. C. and Trolier, M. 1995. Changes in oceanic and terrestrial carbon uptake since 1982. *Nature* **373**, 326–330.

Fung, I., Prentice, K., Matthews, E., Lerner, J. and Russell, G. 1983. Three-dimensional tracer model study of atmospheric CO_2: response to seasonal exchanges with the terrestrial biosphere. *J. Geophys. Res.* **88**, 1281–1294.

Fung, I. Y., Tucker, C. J. and Prentice, K. C. 1987. Application of advanced very high resolution radiometer vegetation index to study atmosphere-biosphere exchange of CO_2. *J. Geophys. Res.* **92**, 2999–3015.

Gaudry, A., Monfray, P., Polian, G., Bonsang, G., Ardouin, B., Jegou, A. and Lambert, G. 1991. Non-seasonal variations of atmospheric CO_2 concentrations at Amsterdam Island. *Tellus* **43B**, 136–143.

Heimann, M., Keeling, C. D. and Tucker, C. J. 1989. A three-dimensional model of atmospheric CO_2 transport based on observed winds (3). Seasonal cycle and synoptic time scale variations. Aspects of climate variability in the Pacific and the Western Americas. *Geophysical Monograph* **55**, ed. D.H. Peterson, AGU, Washington (USA), 277–303.

Houghton, R. A. 1991. Tropical deforestation and atmospheric carbon dioxide. *Climatic change* **19**, 99–118.

Keeling, C. D., Bacastow, R. B., Carter, A. F., Piper, S. C., Whorf, T. P., Heimann, M., Mook, W. G. and Roeloffzen, H. 1989a. A Three-dimensional Model of Atmospheric CO_2 transport based on observed winds (1). Analysis of Observational data. Aspects of climate variability in the Pacific and the Western Americas. *Geophysical Monograph* **55**, ed. D.H. Peterson, AGU, Washington (USA), 165–236.

Keeling, C. D., Piper, S. C. and Heimann, M. 1989b. A three-dimensional model of atmospheric CO_2 transport based on observed winds (4). Mean annual gradients and interannual variations. Aspects of climate variability in the Pacific and the Western Americas. *Geophysical Monograph* **55**, ed. D.H. Peterson, AGU, Washington (USA), 305–363.

Keeling, C. D. and Whorf, T. P. 1994. Atmospheric CO_2 records from sites in the SIO air sampling network. *Trends '93. A Compendium of data on global change*, ed. T.A. Boden, D.P. Kaiser, R.J. Sepanski, F.W. Stoss, Carbon Dioxide Information Analysis Center, Oak Ridge, U.S.A., 16–26.

Law, R., Simmonds, I. and Budd, W. F. 1992. Application of an atmospheric tracer model to the high southern latitudes. *Tellus* **44B**, 358–370.

Law, R. M. 1993. *Modelling the global transport of atmospheric constituents.* PhD thesis, School of Earth Sciences, University of Melbourne, Australia, 204pp.

Nakazawa, T., Miyashita, K., Aoki, S. and Tanaka, M. 1991. Temporal and spatial variations of upper tropospheric and lower stratospheric carbon dioxide. *Tellus* **43B**, 106–117.

Newell, R. E. and Weare, B. C. 1977. A relationship between atmospheric carbon dioxide and Pacific sea surface temperatures. *Geophys. Res. Lett.* **4**, 1–2.

Newell, R. E., Navato, A. R. and Hsiung, J. 1978. Long-term global sea surface temperature fluctuations and their possible influence on atmospheric CO_2 concentrations. *Pure App. Geophys.* **116**, 351–371.

Pearman, G. I. and Beardsmore, D. J. 1984. Atmospheric carbon dioxide measurements in the Australian region: 10 years of aircraft data. *Tellus* **36B**, 1–24.

Rayner, P. J. and Sarmiento, J. L. 1993. CO_2 Budgets in the atmosphere inferred from general circulation models. *Proceedings of the 4th International CO_2 Conference*. Carqueiranne, France, 13–17 September, WMO, 125–128.

Rayner, P. J. and Law, R. M. 1995. *A comparison of modelled responses to prescribed CO_2 sources.* CSIRO Div. of Atmos. Res. Tech. Paper No 36/CRC Sthn. Hem. Met. Tech. Rep. No 1, 82pp.

Reynolds, R. W. 1988. A real-time global sea surface temperature analysis. *J. Climate* **1**, 75–86.

Simmonds, I. 1985. Analysis of the 'spinup' of a general circulation model. *J. Geophys. Res.* **90**, 5637–5660.

Simmonds, I., Trigg, G. and Law, R. 1988. *The climatology of the Melbourne University general circulation model.* Pub. no. 31, Department of Meteorology, University of Melbourne, 67pp. [NTIS PB 88 227491.]

Takahashi, T. 1989. The Carbon Dioxide Puzzle. *Oceanus* **32**, 22–29.

Tans, P. P., Conway, T. J. and Nakazawa, T. 1989. Latitudinal distribution of the sources and sinks of atmospheric carbon dioxide derived from surface observations and an atmospheric transport model. *J. Geophys. Res.* **94**, 5151–5172.

Tans, P. P., Fung, I. Y. and Takahashi, T. 1990. Observational constraints on the global atmospheric CO_2 budget. *Science* **247**, 1431–1438.

Thompson, M. L., Enting, I. G., Pearman, G. I. and Hyson, P. 1986. Interannual variation of atmospheric CO_2 concentration. *J. Atmos. Chem.* **4**, 125–155.